International Journal of Electrospun Nanofibers and Applications, Vol. 4, No. 1 (January-June, 2018)
ISSN : 0973-628X

A Visualization Technique for Mapping the Velocity of Raising Fibers Production in an Electrostatic Field

D. Jašíková* & V. Kopecký

Institute of System Control and Reliability Management, Technical University of Liberec
Czech Republic

Abstract*. Presented here is a novel approach for the visualisation and velocity measurements of polymer jet behavior under an electrostatic field using particle image velocimetry method (PIV). Electrostatic spinning is a process applying a high voltage field for the production of 1 μm – 100 nm fibers. Here we use a PIV technique to map the polymer jet motion, analyzing the velocity of raising fibers and their characteristic movements. Various concentrations of polymer PVA 88 - 08 were observed and compared, showing the relationship between polymer viscosity and velocity factor linking directly to the real time fiber production.*

Keywords: *Electrospinning, nanofibres, PIV system, experimental measurement technique*

1. INTRODUCTION

The fabrication process of very fine polymer fibres using electrostatic spinning has been widely studied in recent years [1]. The use of nanofibres (NF) has many potential applications such as scaffolds for tissue engineering, wound healing, affinity membranes and recovery of metal ions, release control, catalyst and enzyme carriers, sensors or energy storage. As the production process is complex and chaotic due to the high velocity and random motion of the NF within the electrostatic field during spinning such application can not be fully realised [2-4].

Commercial applications require the NF to be completely evaporated, highly organised with uniformed diameters when deposited onto the matrix. To date the fibre jet behaviour and its forming within the field has not been fully described. Research into mapping the production of NF is of great interest at present with studies on the morphology of raising fibres and testing of polymer spinnebility, the influence of the shape of the electrostatic field and external stimuli such as applied voltage or magnetic field in an attempt to optimise the processing technique [5-7].

Electro spinning is an electrostatically induced self-assembly process that can continuously produce ultra-fine fibres with nanoscale diameters through the action of an external electric field imposed on the polymer solution. The general electrospinning apparatus consist of a syringe (Fig. 1), with a small orifice to its edge, high voltage power supply and a grounded target.

* Corresponding author: *darina.jasikova@tul.cz*

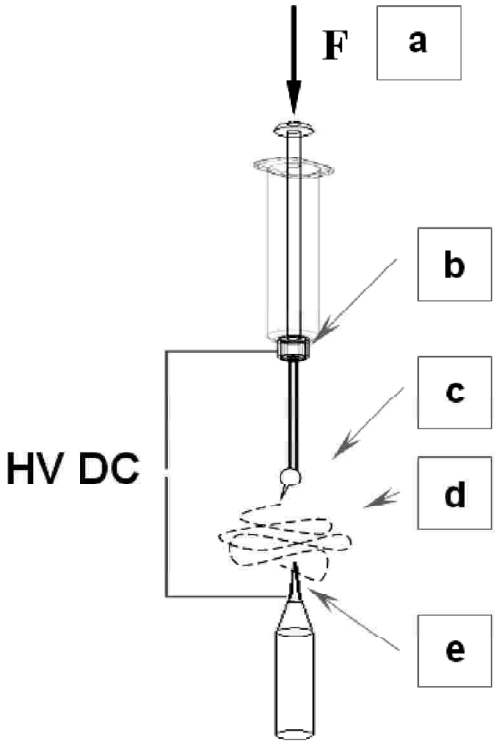

Figure 1: Force *F* (a) Developed by The Syringe Pump and High Voltage (b) is Applied. This Causes the Breakdown of The Surface Tension Forces (c) and The Polymer Jet Passes Through Electrostatic Field (d) with High Velocity and Chaotic Motion Towards The Collector (e)

The syringe is filled with the polymer solution and a voltage is applied by attaching a metal electrode [Fig. 1(b)] to the voltage source. Charge is induced on the liquid surface by the electric field. Mutual charge repulsion causes a force directly opposite to the surface tension. As the intensity of the electric field is increased, the hemispherical surface of the solution at the tip of the capillary tube elongates to form a conical shape known as the Taylor cone [8]. When the electric field reaches a critical value at which the repulsive electrical forces overcome the surface tension forces, a charged jet of the solution is ejected from the tip of the Taylor cone [Fig 2]. The charge in the polymer solution has to be high enough to overcome the surface tension [Fig 1(c)]. As the jet travels in air, the solvent evaporates, leaving behind a charged polymer fibre. The charged jet undergoes stretching and bending, resulting in the formation of many continuous NF. These continuous NF are collected in the form of a non-woven fabric. The polymer jet accelerates through the electrostatic field from the tip of the needle towards the collector with the fibre being elongated [Figs 1(d) - 1(e)]. To use this process for commercial applications the ability to fully characterise the polymer fibre from the droplet to the collector would be crucial for any optimisation [9].

Figure 2: Photograph of Electrostatically Spinned Fibres 14% Concentrated Polyvinyl Alcohol. This Image was taken with Nikkon D70 Camera at a Shutter 250 ms Using a Nikkor Makro 60 Lens, Using Laboratory Needle Spinner and Rounded Disk as a Collector Fixed in a Distance 60mm From A Needle Tip, with Applied Voltage 14kv

This article focuses on fibre visualisation using *particle image velocimetry* PIV method. This is commonly used for the dynamical mapping of fluidic motion [10]. Presented in this paper is a novel approach of mapping the behaviour of the polymer jet in an electrostatic field and relating this to the viscosity of the polymer solution.

2. EXPERIMENTAL SETUP

Polyvinyl alcohol (Mowiol 88 – 08, Mw = 67,000 purchased from Clariant GmbH, Germany) is used without any further purification. This was dissolved into distilled water, gently stirred for 2 h at 90°C to form homogeneous concentrations of 8, 10 and 12% in mass. Material properties of each concentration give the refractive index as 1.340, 1.347 and 1.350 and viscosities of 60, 100 and 200 $mPas^{-1}$ at 20°C for fully hydrolysed solution [11-15].

A 50μl Hamilton syringe reservoir using an edgeless grinded needle of gauge 23 was loaded with the various polymer solutions and connected to a single syringe

pump with a controlled feed-rate of 10µl/min. This was in turn connected to the positive high voltage power supply (FX50P06, Glassman High Voltage) with an applied the voltage of 8.2 kV. A grounded sharp steel tip was placed at 50 mm from the needle [Fig. 1(e)] for fibre collection.

The classical well known particle image velocimetry (PIV) system is one of the oldest techniques for non – invasive studying of velocities in a fluid [8]. This requires seeding particles which are illuminated by a thin sheet of light, and tracked using a laser and CCD camera to give information about the local fluid movement [Fig. 3]. The seeding particles are small with their specific weight close to that of the fluid, so not to disrupt the flow. Images are taken with a time step and cross correlated to produce a velocity profile of the fluid.

To apply these commonly used micrometer diameter particles to NF production would lead to dramatic changes in the hydro dynamical process of the polymer jet. This might be mainly caused by the opposite polarized seeding particles charge and also disruption instabilities in a polymer solution structures. Thus a new approach to use the polymer itself to form the seeding particles is applied here. For each concentration of polymer exists an optimal set up, balancing the complex interactions of fluid flow, electrical forces and solvent evaporation, that leads to a smooth fibre production [Fig 4(a)] and [Fig 4(b)].

If the optimal voltage is set and feedrate is slightly modified, instability at the surface of the rising fibres will occur. If properly controlled, beads are formed within

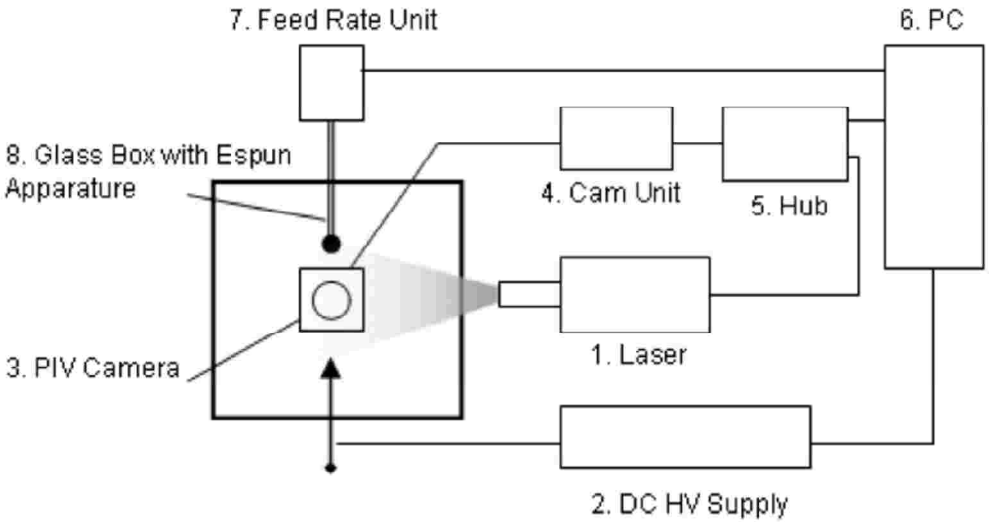

Figure 3: Experimental Setup, 1. Laser New Wave Gemini PIV, 16Hz max., 2. DC HV Supply Glassman, max 50 kV possitive, 3. PIV Camera Dantec HiSense 12bit, 1280×1024, 4.5 double-frames/sec max, Lens System Nikon AF Nikkor 60mm, 4. Camera Unit Dantec Camera Controller, 5. Dantec System Hub – Flowmap, 6. PC for Synchronization, 7. Feed Rate Unit with Controlled Feed Rate 5 – 200ul/min, 8. Glass Box with Electro-spinning Apparature, Distance between Electrodes 50mm

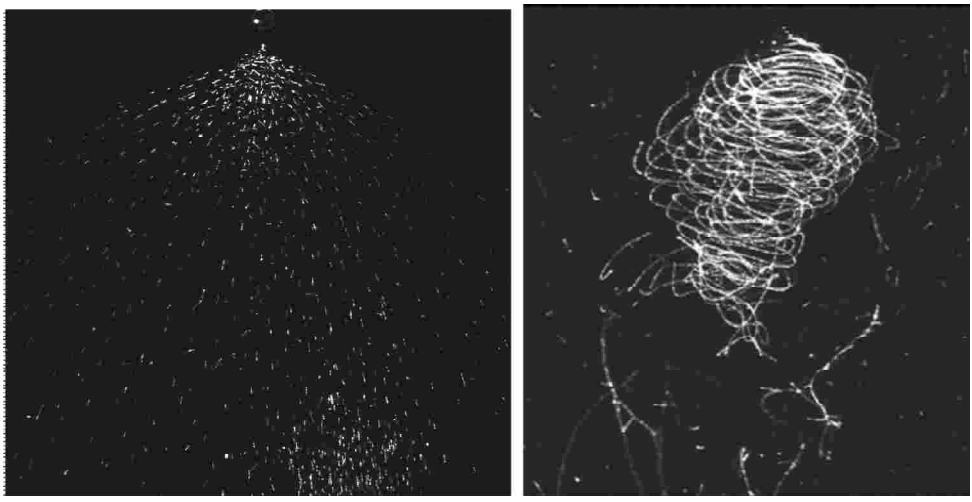

Figure 4a: Images of Nanofibres. A Surface Tension and The Viscosity of the Polymer Solution Influence the Fibre's Behaviour in Electrostatic Field. The Picture (a) Shows the Fibres in the Laser Sheet that are Oriented among the Streamlines. Such a Fibres are Smooth and Straight, Leads to Highly Oriented Structures on a Collector. (b) Low Viscose Polymer Solution is mostly Rotate Round the Central Axis of the Polymer Jet. This Behaviour is mostly Visualized. [18] This Behaviour is Chaotic and Accidentally Oriented Layers with High Range of Instabilities in Structure

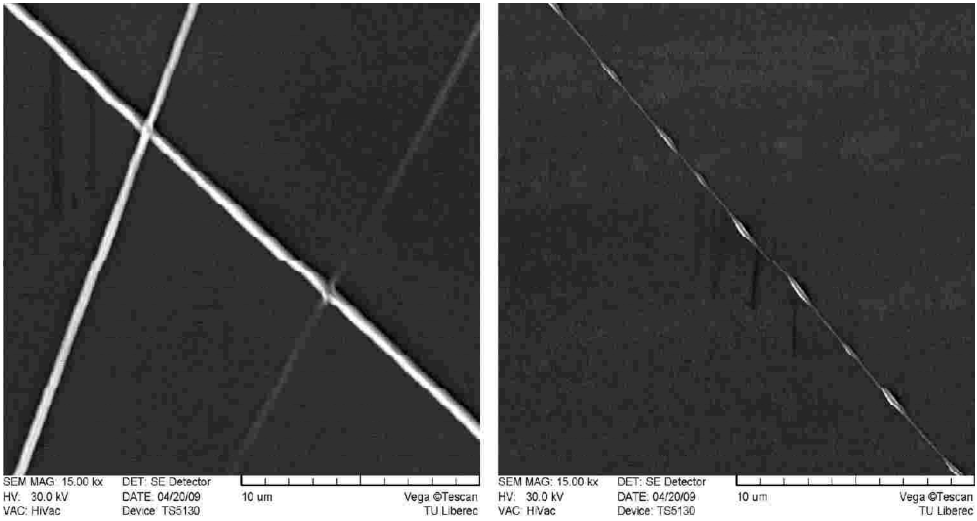

Figure 4b: SEM Image of PVA Fibres. (a) Smooth 12% PVA Nanofibres of 250nm Diameter. (b) 10% PVA Nanofibres of 150nm with Beads of Diameter 1.5 μm

the polymer [16 - 18] as seen in as seen in figure 4b. The NF diameter and beads distributions were determined using an LUCIA image analyzer. The morphology of the NF is observed using a scanning electron microscopy (SEM, Vega, Tescan) for

smooth and beaded NF respectively [Fig. 4(a)] and [Fig.4 (b)]. The beads are seen to have a regular ellipsoidal shape and near constant diameter of 400 nm. The lengths are measured to be 3 µm to 0.5 µm for NF diameters of 200 nm to 100nm respectively. The distances between beads are 5.0 µm for an 8% concentration decreasing to 4.0 µm for a 10% contraction [Fig. 5, 6]. The feedrate of solution into the process was approximately raised in 2% from optimal value that leads to smooth fibres, for each polymer solution according to aperture setup.

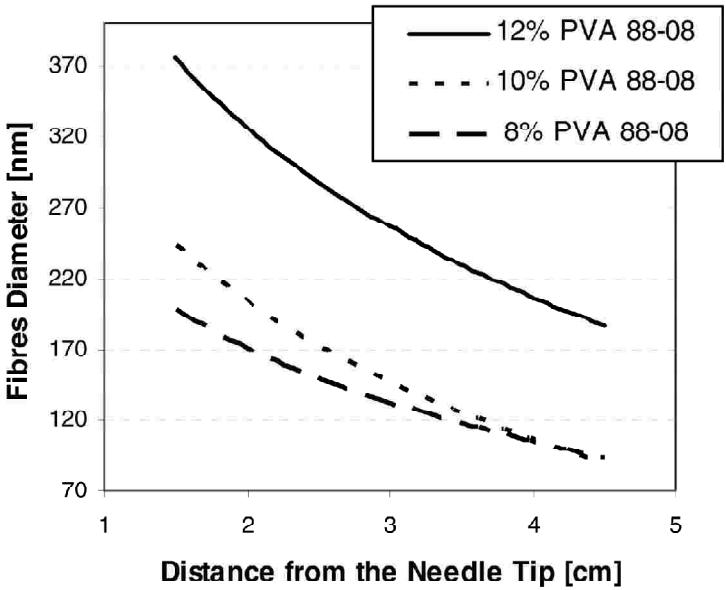

Figure 5: Fibres Diameter Changes with the Distance from the Needle Tip for Polyvinyl alcohol – Mowiol 88 – 08 under 8, 10 and 12% Concentrations

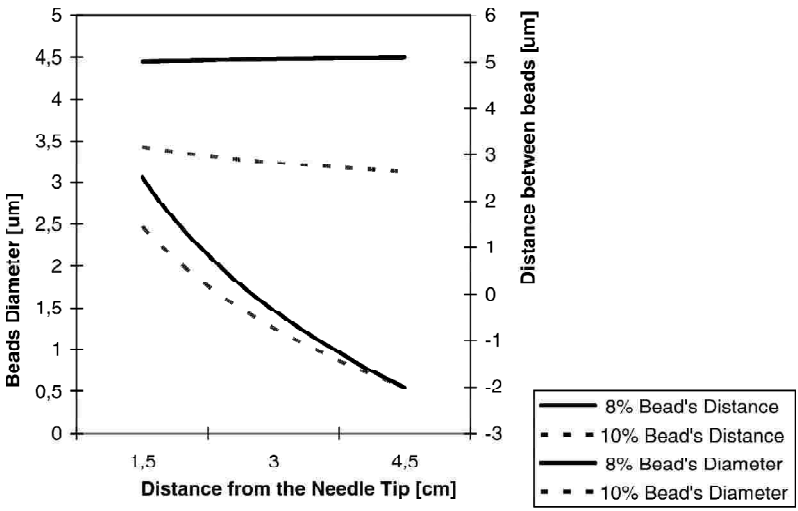

Figure 6: Beads Changes Corresponding with Fig. 5 – Changes of Fibers Diameter

The jets visualisation is processed using a Nd:YAG pulse laser with a HighSense camera placed orthogonal to the incident plane of the beam. Figure 2(a) shows that the fibres are visible by refraction due to the fibre itself bending in the electrostatic field, however, this is limited, requiring the fibre to be in a specific position to the laser. With the introduction of the spherical beads [Fig. 7(a)] and [Fig. 7(b)], the fibre orientation is not required as the beads form the source of the refraction. As the fibre and beads are one system, the refraction image highlights the complete fibre motion. To ensure accurate cross collection a time step of 500 ms is used between images. In this case we are using Nd:YAG pulse laser of wave length 532nm for the fibres visualization. This wave length can easily visualize fibres and beads in diameter up from 600nm. This hypothesis corresponds with the rules of Mie light scattering theory. Fibres with diameter below this value of laser light wave length are for CCD camera invisible.

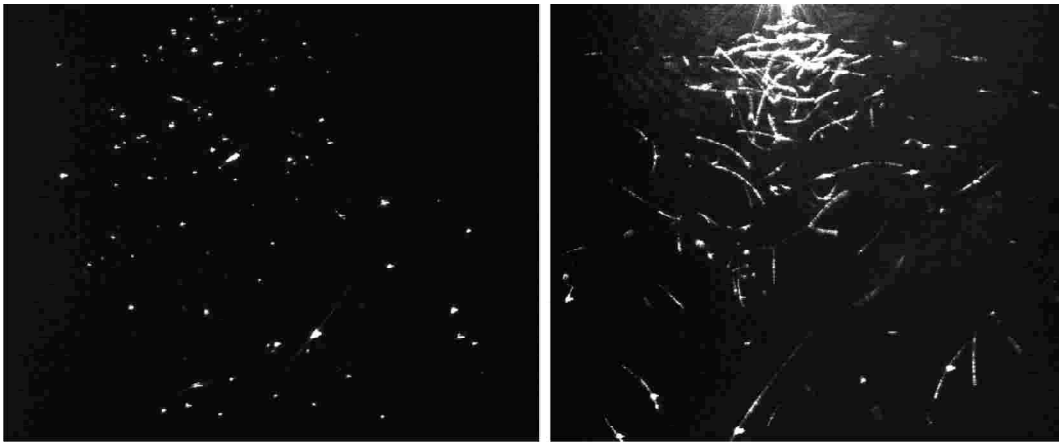

Figure 7: (a) Visualization of Smooth 12% PVA Nanofibres of Diameter from 380 – 200nm towards the Collector. (b) Visualization of 10% PVA Nanofibres of Diameter from 250 – 100 nm with Beads of Diameter 2.5 – 1 μm. These Pictures were taken using HighSense Camera – Part of the PIV Measuring System. Fibres are Visualized with a Laser Sheet of width 5mm using Nd:YAG Pulse Laser of Wavelength 532nm

3. RESULTS AND DISCUSSION

Using the PIV method, image pairs were taken and cross correlated in the optimal selected interrogation area. This is required to be maintained across the image to keep the same space resolution of the vector map results. Applied to the raw vector maps are validation methods (peak, range validation) to normalize the vectors. This is then averaged over 150 different vector maps to produce the final scalar vertical velocity map of the polymer fibers motion in an electrostatic field [Fig. 8]. The fiber jet experiences a large acceleration, reaching the highest velocity (2.8 ms^{-1}) near the needle tip [Fig. 8(a)]. This is caused by a local maximum intensity of the electrostatic field and electrical forces which are greater than the intermolecular forces of the polymer.

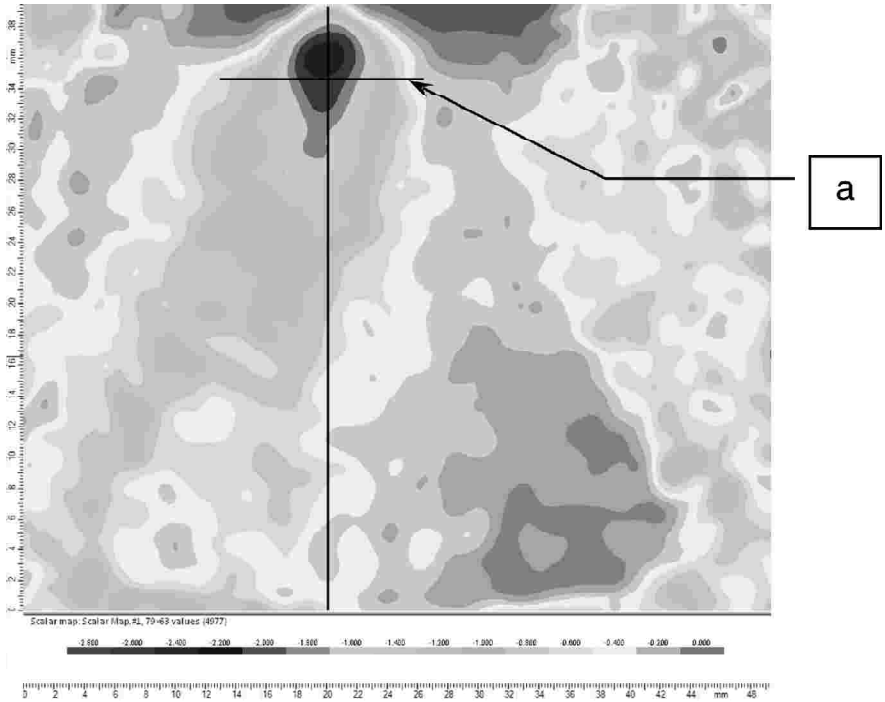

Figure 8: Scalar Map of y – axis Fibers Motion Velocities towards the Collector. The Region with the Highest Velocities are Dark Coloured. The Maximum Velocity in this Region is 2.2 m/s. The Symmetric Opposite Velocities among Central Axis are caused by the Rotation of Polymer Jet. a) The Line Scan for Calculation of Velocity Profiles for Various Concentrations of Polymer Solutions that are Compared Below

Moving through the field the fiber jet motion is stagnated and accelerated again as it becomes closer to the opposite charged collector.

A velocity profile can be created by taking a line scan of the scalar map indicated as the line (a) in figure 8. Figure 4 highlights the velocity for three polymer concentrations of 8%, 10% and 12% in mass. The velocity can be then linked to the material properties such as viscosity. A higher polymer concentration that is more viscous for most polymer solutions, where the molecular chain is highly tangled, such as a 12% mix, shows a lower velocity in the electrostatic field. This is conversely true whereby a lower viscose material with less tangled molecules exhibits a higher velocity such as in the 8% concentration [Fig. 9].

4. CONCLUSION

Presented here is a novel way of the visualisation of a polymer jet using a modified PIV method. Using cross collected images the velocity of NF can be plotted as they move through the electrostatic field allowing a high resolution non invasive mapping of the NF production.

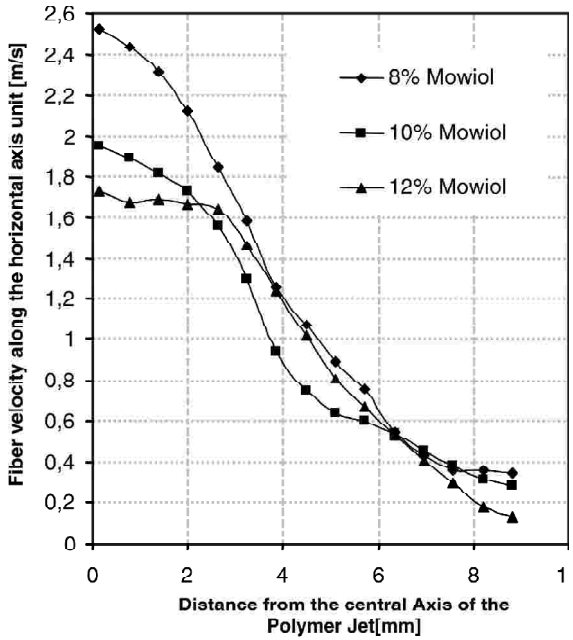

Figure 9: **Polymer Jet Velocity Profile for Concentration 8%, 10% and 12% in Mass. This Profile is Symmetric Along the y – axis. In all cases the Applied Voltage was 8.2 kV with an Electrode's Distance of 50mm**

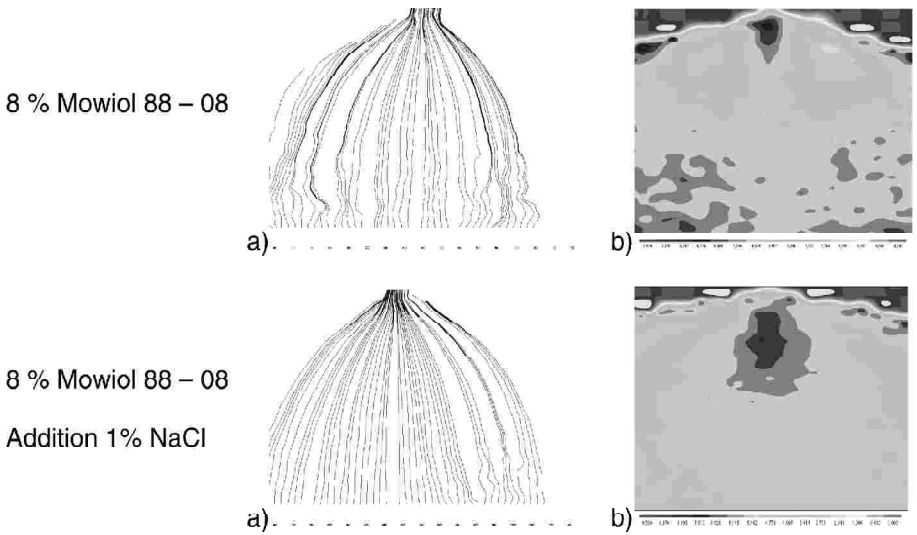

Figure 10: **The Applicaton of the PIV Visualization and Calculation Method on the Raising Conductivity Event. In this Case a Very Short Fibres are Produced (a) The Streamlines of the Fibres Motion (b) The Scalar Map of a Velocity Distribution. The Dark Blue Color Marks the Maximum Velocity – 6,8 m/s. This Velocity was reached on Experimental Setup of 60mm Gap Between the Electrodes and Applied Voltage 14kV**

This new technique can be used to link the polymers material properties to its flow in production leading to a detailed velocity map for each concentration with higher resolution non invasive mapping of the NF production. This would open the door to forming new NF structures and processing techniques in situ for many new applications. The velocity scalar map can also be used to observe the effects of external stimuli applied to the electrostatic field, such as magnetic fields, electrostatic lens and other ambient factors.

ACKNOWLEDGEMENTS

The authors are grateful to Prof. D. Lukáš, D. Zálesákova and J. Farberova from Department of Nonwovens for their advices and support.

References

[1] S. Ramakrishna, K. Fujihara, W. E. Teo, T. Ch. Lim, Z. Ma, *An Introduction to Electrospinning and Nanofibers*, 1st ed.(World Scientific Publishing Company, 2005).

[2] J. Venugopal, S. Ramakrishna, *Applied Biochemistry and Biology* 125, 147 (2005).

[3] Ch. P. Poole, *Introduction to Nanotechnology* (Wiley, Hoboken, 2003).

[4] J. Fang, T. H. Niu, T. Lin, and X. G. Wang, *Chinese Science Bulletin* 53, 2265 (2008).

[5] C. S. Kong, T. H. Lee, S. H. Lee, H. S. Kim, *J. Mater. Sci.* 42, 8106 (2007).

[6] N. Savage, M. S. Diallo, *Journal of Nanoparticle Research* 7, 331 (2005).

[7] S. De Vrieze, T. Van Camp, A. Nelvig, et. Al., *J. Mater. Sci.* (online published) (2008).

[8] A. L. Yarin, S. Koombhongse, D. H. Reneker, *J. Appl. Phys.* 89, 3018 (2001).

[9] A. A. Shutov, *Fluid Dynamics* 41, 901 (2006).

[10] R. J. Adrian, *Experiments in Fluids* 39, 159 (2005).

[11] M. Matsumoto, Y. Ohynagi, *J. Polym. Sci.* 26, 389 (1957).

[12] T. Matsuo, H. Inagaki, *Makromol. Chem.* 53, 130 (1962).

[13] K. Amaya, R. Fujishiro, *Bull. Chem. Soc. Japan* 29, 361 (1956).

[14] K. Amaya, R. Fujishiro, *Bull. Chem. Soc. Japan* 29, 830 (1956).

[15] H. Maeda, T. Kawai, S. Seki, *J. Polym. Sci.* 35, 288 (1959).

[16] R. V. N. Krishnappa, K. Desai, S. Changmo, *J. Mater. Sci.* 38, 2357 (2003).

[17] G. Eda, S. Shivkumar, *J. Mater. Sci.* 41, 5704 (2006).

[18] D. H. Reneker, A. L. Yarin, *Polymer* 49, 2387-2425 (2008).